2017 IEEE Conference on Control Technology and Applications (CCTA)
August 27-30, 2017. Kohala Coast, Hawai'i, USA

Lane Centering Assistance system design for large speed variation and curved roads

Iris Ballesteros-Tolosana[1,2], Pedro Rodriguez-Ayerbe[1], Sorin Olaru[1], Renaud Deborne[2], Guillermo Pita-Gil[2]

***Abstract*— The present paper is dedicated to the Advanced Driving Assistance Systems (ADAS). The first goal is to offer an outlook of ADAS which represents a widespread feature of the modern vehicles. After this general perspective, the attention is focused on one of the lateral dynamics control systems, the Lane Centering Assistance system. A Linear Parameter-Varying (LPV) model comprising the most relevant system dynamics is considered with the curvature of the road representing a bounded parameter-varying disturbance. This model will be used for the design of an input-to-state stable LPV observer-based controller within the Linear Matrix Inequality (LMI) framework, ensuring systems' performance in the presence of speed variation and curved roads. In addition, constraint satisfaction and the maximization of the domain of attraction are considered, in order to provide a certified region of operation. As a last part of the study, in order to reduce the conservativeness introduced by large parameter variations, a discontinuous multiple parameter-dependent design is proposed, and stability of the LPV closed-loop switching system is proved by exploiting the dwell time conditions inherited from the hysteresis implementation.**

I. Introduction

Driving is progressively evolving towards a new concept where the human becomes a pure passenger of the vehicle and the control systems are in full charge of the driving task. There exists already an important amount of prototypes and projects that proof that the concept is achievable [1]. Nevertheless, in order to fully offer this kind of technology at an affordable price to the general public, the technique needs to gain in maturity and to be comforted by a secure legal framework. In this framework, the automotive industry is advancing gradually, starting from a novel driving experience and safety enhancements denoted as Advanced Driving Assistance Systems (ADAS). This kind of systems can be considered as a first generation of assisted or semi-autonomous driving, that will pave the way to fully automated vehicles [2]. When speaking of these ADAS systems, one can expect the vehicle to be in charge of certain driving tasks, not at all levels of decision but at certain delimited scenarios and always under human supervision.

Despite this enclosed context, it is a critical feature to design robust control systems that ensure a correct behavior under system's variation of parameters or in the presence of uncertainty. Moreover, from the control point of view, not all the system states are measured via the available instrumentation (Section III-E), so it is necessary to estimate certain internal states. In the present work, vehicle speed and curvature of the road variations are considered at the design stage, in order to compute a suitable observer-based feedback controller that ensures performance under these changes on the driving conditions and system limitations, that are translated into control design constraints. The main contribution of the paper is methodological and proves that an integrated design can cope with a large range of parameter variation and could provide certification for the safety and other constraints on the closed-loop functioning.

The remaining of this paper provides a general overview of the ADAS systems (Section II). Then, Section III is in charge of characterizing the Lane Centering Assistance (LCA) system, which is the target application of the present paper. Then, in Section IV this is used to compute a suitable observer-based LPV feedback controller. After that, design flexibility is enhanced in Section V by means of a LPV switching strategy. Finally, numerical simulations are provided in Section VI and conclusions and further directions are drawn in Section VII.

II. ADAS – brief review

Initial realizations of driving assistance were mostly based on passive components whose main idea was to warn the driver or briefly correct vehicle's trajectory. Here we can name the Blind Spot Warning (BSW), Lane Departure Warning (LDW) or the Lane Keeping Assistance (LKA) [3] systems. In the subsequent, more complex systems have been developed, were the main objective is focused on the complete automation of different driving tasks to improve the drivers comfort and safety. Some of these systems are the Parking Assistance, Automatic Emergency Braking (AEB), Longitudinal dynamics control, Lateral dynamics control or Lane Change Assistance systems.

First versions of Parking Assistance systems have been mostly focused on the steering wheel control, while the driver was still in charge of controlling the longitudinal movement by accelerating or braking as needed. After that, more recent developments are completely capable of executing the maneuver, without any human intervention.

In addition, a huge improvement on the vehicle's safety has been provided by the development of the Automatic Emergency Braking [4]. In a nutshell, this kind of systems are in charge of braking the vehicle if the driver fails to react facing a longitudinal collision. More evolved systems will include obstacle avoidance, like pedestrians, bicycles or other vehicles, that may arise provoking hazardous situations both for the vehicle or the environment [5].

[1] Laboratory of Signals and Systems (L2S), Centrale-Supèlec, CNRS, Université de Paris-Saclay, France. {sorin.olaru, pedro.rodriguez}@centralesupelec.fr
[2]RENAULT SAS {iris.ballesteros-tolosana, renaud.deborne, guillermo.pita-gil}@renault.com

Longitudinal dynamics control is a mature field [6], where the main objective is to regulate vehicle speed and longitudinal distance with the surrounding vehicles. This kind of systems, commonly known as Adaptive Cruise Control (ACC) systems, are already offered by many car manufacturers, and seem to have been successfully accepted by the customers.

Then, lateral dynamics control has been also subject of several studies for a long time [7], [8]. Nevertheless, drivers acceptance of these kind of assistance systems seems to be more troublesome and needs a longer period of time to be completely settled on the market [9]. In principle, the main purpose of these systems is to control the steering wheel of the vehicle, considering different driving objectives. Here we recall the Auto-steer system, whose main purpose is to follow a vehicle that is in front of the controlled one at low speed [10]. Then, the Lane Centering Assistance (LCA), which is in charge of following the center of the lane, considering a broad range of vehicle speed. This is the target system of the present paper, and will be further studied in detail from the modeling stage up to the control design and analysis in view of performance certification.

Lastly, we have the Lane Change assistance, which has been already studied in several research work but in practice still remains a challenge for the real-life application, mostly due to the inherent complexity of the interaction with the surrounding dynamical environment [11].

III. LCA System Model

This section provides a model that allows to describe the LCA system dynamics. Such a model comprises the most representative characteristics of the vehicle lateral dynamics behavior, as well as system actuator dynamics and the influence of the curvature of the road. As a complement and a very important aspect of the deployment, an overview of vehicle's relevant instrumentation is given, defining which are the measured and the estimated states of the system.

A. Lateral vehicle dynamics

The study of vehicle dynamics has been the object of research in different fields and there exists a wide variety of publications like [12], [13], that provide a complete background on the topic and allow to understand deeply the interactions of this system with the environment. Regarding auto-steering applications under regular driving conditions, several assumptions are commonly accepted. It is worth mentioning that in consideration of small side slip angles, the interacting forces between the tyres and the ground are restricted to their linear region [14]. Moreover, decoupled dynamics between the lateral and longitudinal movement is considered in the present paper. Nevertheless, readers are referred to [15], [16], for auto-steering applications under more extreme driving conditions or coupled longitudinal and lateral vehicle dynamics modeling.

In the subsequent, a two degrees of freedom lateral dynamics model is presented. We start from the widely accepted *bicycle model* [8] where each pair of wheels situated at the same axis is merged together. When dealing with lane centering applications, it becomes of interest to do a change of reference, expressing some of the model states with respect to the road. In this way, the following change of coordinates has been considered

$$\dot{\psi}_{rel} = \dot{\psi} - \dot{\psi}_{road} = \dot{\psi} - v_x \rho, \qquad \dot{y}_{CoG} = \dot{y} - v_x \psi_{rel} \quad (1)$$

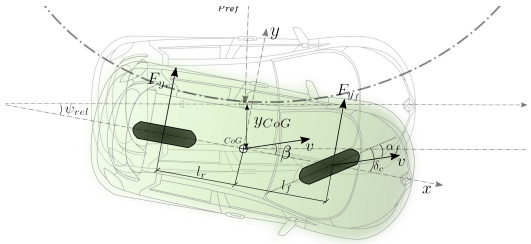

Fig. 1: LCA scheme

The resulting dynamical model is shown in the following:

$$\begin{aligned} \dot{x}(t) &= A_1(v_x(t))x(t) + B_1 u(t) \\ y(t) &= C_1 x(t) \end{aligned} \quad (2)$$

with:

$$A_1(v_x(t)) = \begin{bmatrix} \frac{-(C_f l_f^2 + C_r l_r^2)}{I_z v_x(t)} & \frac{(C_f l_f - C_r l_r)}{I_z} & \frac{-(C_f l_f - C_r l_r)}{I_z v_x(t)} & 0 \\ 1 & 0 & 0 & 0 \\ \frac{(C_r l_r - C_f l_f)}{m v_x(t)} & \frac{(C_f + C_r)}{m} & \frac{-(C_f + C_r)}{m v_x(t)} & 0 \\ 0 & 0 & 1 & 0 \end{bmatrix} \quad (3)$$

$$B_1 = \begin{bmatrix} \frac{C_f l_f}{I_z} & 0 & \frac{C_f}{m} & 0 \end{bmatrix}^T \qquad C_1 = \begin{bmatrix} 1 & 0 & 0 & 0 \\ 0 & 1 & 0 & 0 \\ 0 & 0 & 0 & 1 \end{bmatrix}. \quad (4)$$

The state vector $x \in \mathbb{R}^{n_x}$ is defined together with the control input $u \in \mathbb{R}^{n_u}$ and the measured outputs $y \in \mathbb{R}^{n_y}$ by the following sequence of system states, depicted in Table I.

$$\begin{aligned} x &= \begin{bmatrix} \dot{\psi} & \psi_{rel} & \dot{y}_{CoG} & y_{CoG} \end{bmatrix}^T \\ y &= \begin{bmatrix} \dot{\psi} & \psi_{rel} & y_{CoG} \end{bmatrix}^T \\ u &= \delta \end{aligned} \quad (5)$$

TABLE I: Bicycle model states description

State	Description
$\dot{\psi}$	Rate of change of vehicle orientation (yaw rate)
ψ_{rel}	Heading angle with respect to the road center line
$\dot{y}_{CoG}$	Lateral speed with respect to the road center line
y_{CoG}	Lateral offset with respect to the road center line
δ	Front wheel steering angle
ρ	Curvature of the road (See Section III-B)

System matrices $A_1(v_x(t)) \in \mathbb{R}^{n_x \times n_x}$, $B_1 \in \mathbb{R}^{n_x \times n_u}$ and $C_1 \in \mathbb{R}^{n_x \times n_y}$ depend on several vehicle constants and parameters, described in Table II. In addition to these known and fixed elements, the longitudinal speed of the vehicle $v_x(t)$ appears in several terms of the transition matrix $A_1(v_x(t))$. Let us define the parameter $\gamma(t) = 1/v_x(t)$ as the inverse of the vehicle speed. It is straightforward to notice that the system matrix $A_1(\gamma(t))$ depends linearly on this parameter, whose value is provided by the longitudinal

TABLE II: Vehicle parameters definition

Parameter	Description
C_f	Equivalent cornering stiffness of the front wheels [N/rad]
C_r	Equivalent cornering stiffness of the rear wheels [N/rad]
l_f	Longitudinal distance between CoG and front wheels axis [m]
l_r	Longitudinal distance between CoG and rear wheels axis [m]
I_z	Vehicle moment of inertia along the vertical axis [kgm^2]
m	Vehicle total mass [kg]
v_x	Longitudinal speed of the vehicle

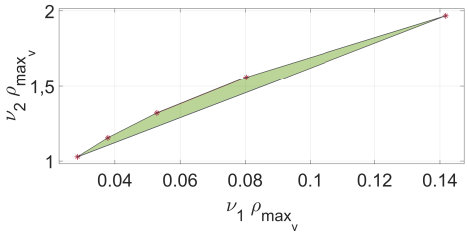

Fig. 2: $E_j(\nu)$ polytopic representation

controller each sample time. Furthermore, it is bounded by the LCA systems predefined range of operation. This means that for control synthesis purposes this measured and bounded variable can be enclosed in a polytope, $\gamma(t) \in \Gamma$. In this respect, we can perform a polytopic decomposition of the system matrix, such that

$$A_1(\gamma(t)) = \sum_{i=1}^{n_v} \xi_i A_{1_i}(\gamma_i(t)) \tag{6}$$

with ξ_i laying in the unit simplex Λ_{n_v} given by $\Lambda_{n_v} = \{\xi_i \in \mathbb{R}^+ : \sum_{i=1}^{n_v} \xi_i = 1, \xi_i \geq 0\}$ and $n_v = 2$. In this way, the following control design problem is translated into a finite set of constraints, that take into account only the vertex of the convex hull of system matrices, $Co\{A_{1_1}, A_{1_2}\}$.

B. Additive disturbances

Next we concentrate on the definition and modeling of the considered additive disturbances for the auto-steering system observer-based controller design. When driving in a dynamical environment, the existing perturbations may be of different nature, being originated from a wide range of sources, like unmodeled dynamics or wind forces [17].

The present paper intends to take into account the effect of the curvature of the road, which has a direct effect on the lateral dynamics of the vehicle by means of the centripetal acceleration that appears when driving in a curve $\ddot{y}_{CoG}(t) = -v_x^2(t)\rho$. In consequence, the required steering wheel angle is directly affected, as we will need to steer as much as it is needed to follow the curve and keep the vehicle centered.

This effect is included in the system dynamics model by means of a bounded additive disturbance, $\rho \in \mathcal{R}$, defined by the disturbances matrix

$$E(v_x(t), v_x^2(t)) = \left[0, -v_x(t), -v_x^2(t), 0\right]^T \tag{7}$$

with $E(v_x(t), v_x^2(t)) \in \mathbb{R}^{n_x \times p}$. It can be seen that this matrix depends on the vehicle speed, thus we have a parameter-varying disturbances matrix.

Moreover, regarding road design standards [18], it can be seen that the maximal admissible curvature value is limited according to the speed. In this way, a polytopic representation of the disturbances matrix is proposed, whose defining vertex E_j are defined by each one of the maximal curve-speed pairs. In this way, the disturbances matrix can be parametrized as a function of a unique parameter, $E_j(\nu(t))$. For a detailed discussion on this topic see [19].

$$E(\nu(t)) = \sum_{j=1}^{\tilde{n}_v} \alpha_j E_j(\nu_j(t)), \tag{8}$$

with α_j laying in the unit simplex $\Lambda_{\tilde{n}_v}$ given by $\Lambda_{n_v} = \left\{\alpha \in \mathbb{R} : \sum_{j=1}^{\tilde{n}_v} \alpha_j = 1, \alpha_j \geq 0\right\}$ and $\tilde{n}_v = 5$. The inclusion of the maximal curvature on the disturbances matrix alows to define a normalized disturbances vector,

$$w_j \in \mathcal{W}_j = \left\{w_j^T w_j \leq 1\right\} \tag{9}$$

C. Steer-by-wire system

In the auto-steering context, it is necessary to actuate on the direction system [20] as the driver would.

In the present work, a steer-by-wire schema is considered. This kind of design is controlled electronically, eliminating any mechanical coupling between the steering wheel and the wheels. Instead, two actuators are installed, generally two electric motors, which are in charge of steering the front wheels and the steering wheel independently. Both actuators are associated, providing the direction, speed and force of the steering wheel and sending it to the steering system at the wheels. In the same way, the driver receives an effort feedback through the steering wheel.

In the following, the actuator dynamics are presented, considering an electric motor under position control, which is part of the steer-by-wire system and that is in charge of transforming the commanded steering angle δ_c into front wheels steering angle δ. This model follows the lines of [21], where a linearized steering actuator model is given by a second order system transfer function. Using a state-space representation, we obtain,

$$\frac{d}{dt}\begin{bmatrix}\dot{\delta}\\ \delta\end{bmatrix} = \underbrace{\begin{bmatrix}-2\xi\omega & -\omega^2\\ 1 & 0\end{bmatrix}}_{A_2}\begin{bmatrix}\dot{\delta}\\ \delta\end{bmatrix} + \underbrace{\begin{bmatrix}\omega^2\\ 0\end{bmatrix}}_{B_2}\delta_c \tag{10}$$

where ξ represents the damping factor and ω stands for for the cut frequency of the modeled dynamics. Numerical values are not included for confidentiality reasons.

D. Full dynamical model

Integrating the elements presented in the previous sections, we can formulate the complete dynamical model in view of control that includes the formulation of the vehicle lateral dynamics with respect to the road, the curvature influence and the actuator behavior. In this way, equations (2), (10) and (7) can be assembled, obtaining a single state-space

representation of the full system dynamics that will be used in Section IV for the observer and controller design:

$$\begin{aligned} \dot{x}(t) &= \bar{A}(\gamma(t))x(t) + \bar{B}u(t) + \bar{E}(\nu(t))w \\ y(t) &= \bar{C}x(t) \end{aligned} \tag{11}$$

where $\bar{A}(\gamma)$, $\bar{B}$, $\bar{C}$, $\bar{E}(\nu)$ are defined by the concatenation of the models presented in Sections III-A, III-B and III-C:

$$\bar{A}(\gamma) = \begin{bmatrix} A_1(\gamma(t)) & B_1 \\ [0] & A_2 \\ A_3 & [0] \end{bmatrix} \quad \bar{B} = \begin{bmatrix} [0] \\ B_2 \\ 0 \end{bmatrix}$$
$$\bar{E}(\nu) = \begin{bmatrix} E(\nu) \\ [0] \\ 0 \end{bmatrix} \quad \bar{C} = \begin{bmatrix} C_1 & [0] & [0] \\ [0] & \begin{bmatrix} 0 \\ 1 \end{bmatrix} & [0] \end{bmatrix} \tag{12}$$

with the following state, output and input vectors

$$\begin{aligned} x &= \begin{bmatrix} \dot{\psi} & \psi_{rel} & \dot{y}_{CoG} & y_{CoG} & \dot{\delta} & \delta & \int -y_{CoG}dt \end{bmatrix}^T \\ y &= \begin{bmatrix} \dot{\psi} & \psi_{rel} & y_{CoG} & \delta & \int -y_{CoG}dt \end{bmatrix}^T \\ u &= \delta_c \end{aligned} \tag{13}$$

It has to be noted that this reformulation includes an integral action on the lateral position of the vehicle with respect to the road, in order to eliminate the steady-state error, with $A_3 = [0, 0, 0, -1, 0, 0, 0]^T$. In the following, system dynamics are discretized by a first order Euler method with $T_s = 10$ms.

Remark 1: It is important to notice that the vehicle and actuator dynamics are modeled in terms of the front wheels steering angle δ. Nevertheless, our actuator and the corresponding sensor are connected to the steering system through a rack. Thus, it is crucial to consider the reduction ratio i_r between the front wheels and the vehicle steering wheel when interacting with the system, sending the control signals $\bar{\delta}_c$ or transforming the received the measurements δ_{meas} in the proper reference, that is, $\bar{\delta}_c = \delta_c i_r$, $\delta = \delta_{meas}/i_r$.

E. Vehicle instrumentation

Generally speaking, we can distinguish between two kinds of sensors, denoted as exteroceptive or proprioceptive.

On one hand, the first type of sensors is in charge of providing environment measurements as well as the relative state of the vehicle. The main exteroceptive sensors for the LCA system include a camera and a radar, which are in charge of providing the position of the vehicle with respect to the lines of the road y_{CoG}, ψ_{rel} as well as the movement and location of the surrounding elements. On the other hand, the second type of sensors has the objective of yielding own vehicle information. Here we include the measurement of the steering angle δ_{meas} by means of a relative or absolute encoder and a gyro for the vehicle yaw rate $\dot{\psi}$. For the rest of LCA non-measured states, an observer that estimates their values is needed (Section IV).

IV. LPV design in the presence of additive disturbances and system constraints

As it has been stated in Section II, the objective of the auto-steering system is to control the vehicle to the center of the the current lane. Due to the fact that the system dynamics have been expressed with respect to the road, such an objective is translated into a stabilization of system dynamics to the origin. This section presents the main theoretical tools that have been used to design an observer-based controller state feedback for the LPV system introduced in Section III in the presence of parameter-varying additive disturbances.

First, the observability of the auto-steering dynamics should be analyzed. Let us consider the first two blocks of the observability matrix $\mathcal{O}_n(\gamma)$ defined as in [12], obtaining $[\bar{C},\ \bar{C}\bar{A}(\gamma)]^T$. From this two blocks, it is possible to obtain a full rank matrix that does no depend on the speed of the vehicle, for example $[\bar{C},\ \bar{C}\bar{A}(\gamma)_{(2:3\times 7)}]^T$, thus, the LCA system is observable no matter the parameter value.

In the remaining of this section, the simultaneous design of a LPV observer-controller is translated in terms of LMI [22], whose resolution provides a suitable tuning that ensures input-to-state stability for a LPV system which is affected by additive disturbances.

Main results from [23] are adapted for the parameter-varying additive disturbances (7), (8) case. Theorem 1 is included here for completeness, but its proof is omitted for the sake of brevity.

Theorem 1: Let us consider a discrete-time LPV system affected by bounded disturbances (9). If there exist $G_i = G_i^T \succ 0$, $P_i = P_i^T \succ 0$, Q_{G_i}, Q_{P_i}, Y_i, Z_i of appropriate dimensions, with $i, l = [1 \dots n_v]$, $j = [1 \dots \tilde{n}_v]$ and $\tau > 0$, $\beta \geq 0$, $\lambda \geq 0$ such that:

$$\begin{bmatrix} Q_{G_i}^T + Q_{G_i} - G_i & 0 & \tau Q_{G_i}^T & Q_{G_i}^T \bar{A}_i^T - Y_i^T \bar{B}^T \\ \star & \beta I & 0 & \begin{bmatrix} \bar{E}_j & 0 \end{bmatrix}^T \\ \star & \star & \tau G_i & 0 \\ \star & \star & * & G_l \end{bmatrix} \succ 0, \tag{14}$$

$$\begin{bmatrix} P_i & 0 & \tau P_i & \bar{A}_i^T Q_{P_i}^T - \bar{C}^T Z_i^T \\ \star & \lambda I & 0 & [Q_{P_i}\bar{E}_j \ -Z_i E_v]^T \\ \star & \star & \tau P_i & 0 \\ \star & \star & \star & Q_{P_i}^T + Q_{P_i} - P_l \end{bmatrix} \succ 0, \tag{15}$$

$$\tau - \beta \geq 0, \tau - \lambda \geq 0,\ i, l = [1 \dots n_v], j = [1 \dots \tilde{n}_v] \tag{16}$$

then the system is input-to-state stable in the case of bounded norm disturbances (9). The feedback and observer gains that stabilize the system are defined by:

$$K_i = Y_i Q_{G_i}^{-1}, \quad L_i = Q_{P_i}^{-1} Z_i, \quad i = [1 \dots n_v]. \tag{17}$$

We can calculate $F(\gamma)$ and $L(\gamma)$ at any working point as a convex combination of the vertex realizations:

$$K(\gamma_k) = \sum_{i=1}^{n_v} \mu_{i_k} K_i(\gamma_i) \text{ and } L(\gamma_k) = \sum_{i=1}^{n_v} \mu_{i_k} L_i(\gamma_i). \tag{18}$$

with $\sum_{i=1}^{n_v} \mu_{i_k} = 1$, $\mu_{i_k} \geq 0$ and $n_v = 2$. ■

Remark 2: It must be noted that Theorem 1 inequalities (14), (15) are Bilinear Matrix Inequalities (BMI) due to the scalar variable τ that multiplies P_i, G_i and Q_G. This kind of problem could be solved with a state-of the-art BMI solver, like PENBMI [24]. Nevertheless, the optimal value of the scalar variable can be obtained in terms of a loop that solves the problem for the whole range of admissible values.

A. Controller robust domain of attraction with constraints

The LPV observer-based feedback controller designed in the previous section ensures system stability in the presence of the parameter variation and bounded additive disturbances. Nevertheless, in this kind of application it is crucial to provide a certified range of operation for the designed LPV controller in the presence of parameter variations, additive disturbances and system constraints. In this way, it is important to delimit the region of the state-space in which the conceived tuning for the LPV system satisfies the system constraints regardless the driving conditions. Such region is approximated by an ellipsoid $\mathcal{E}_G = \{x^T G^{-1} x \leq 1\}$ centered at the origin, that is denominated robust positive invariant (RPI) with respect to the closed loop dynamics if $\forall x \in \mathcal{E}_G$ then $A_{CL}(\gamma)x + E(\nu)w \in \mathcal{E}_G, \forall w \in \mathcal{W}$ and $\forall \gamma \in \Gamma$, with A_{CL} denoting the closed-loop system dynamics [25]. This means that any initial state that belongs to $\mathcal{E}_G$ will satisfy system constraints and not leave the computed admissible set under any (bounded) parameter variation or disturbance. Moreover, this ellipsoid $\mathcal{E}_G$ will be the limit set of all the trajectories of the system controlled with the LPV feedback gain (17). This means that all the trajectories that start on the computed ellipsoid will remain in $\mathcal{E}_G$ with certification of the constraints satisfaction and all the ones starting outside this region will converge to it [23]. Nevertheless, in the later case no certification of constraint satisfaction is provided.

In this lines, based on Theorem 1, we can obtain a suitable robust tuning for system (11), while considering the system constraints and maximizing the RPI ellipsoid size by solving the following optimization problem:

$$\min - logdet(G_i) \tag{19}$$

subject to

- Invariance condition (14), (15), (16).
- Constraints satisfaction [26].
  - On input:

$$\begin{bmatrix} Q_{G_i}^T + Q_{G_i} - G_i & Y_i^T \\ Y_i & u_{max}^2 I \end{bmatrix} \tag{20}$$

  - On output:

$$\begin{bmatrix} Q_{G_i}^T + Q_{G_i} - G_i & Q_{G_i}^T \bar{C}_i^T \\ \bar{C}_i Q_{G_i} & y_{max}^2 I \end{bmatrix} \tag{21}$$

  - On states:

$$\begin{bmatrix} 1 & F_f^T Q_{G_i}^T \\ Q_{G_i} F_f & Q_{G_i}^T + Q_{G_i} - G_i \end{bmatrix} \tag{22}$$

The size of an ellipsoidal set is directly related to the product of the eigenvalues of its shape matrix P^{-1}, which is directly related to its determinant. The operator $logarithm$ is used to obtain a concave problem that afterwards is translated into a convex minimization problem with the sign inversion.

V. LPV SWITCHED CONTROL

Due to the large range of variation on the vehicle speed, it could remain conservative to use a single LPV controller over the whole admissible range of the parameter variation. In order to reduce such conservativeness, it is possible to tune multiple LPV controllers, each one suitable for a defined parameter subspace. This provides more flexibility on the design stage, but global stability of the switched LPV system needs to be checked a posteriori.

In the present paper, two different overlapped switching modes denoted by the subindex $\sigma \in \{\sigma_1, \sigma_2\}$ defining an hysteresis switch [27] have been considered. Each mode will be active at low and high speed respectively. In this way, a discontinuous parameter-dependent Lyapunov function (23) is defined over the range of operation by means of multiple parameter-dependent Lyapunov functions, each one ensuring the closed-loop stability on the active parameter subspace.

$$V_\sigma(x, \gamma) = x^T G_\sigma^{-1}(\gamma) x \tag{23}$$

For the LPV switched closed-loop system working under the hysteresis switching strategy to be stable, the value of the discontinuous Lyapunov function is not necessary decreasing along the whole range of the parameter and may have discontinuities due to the switch [28]. Nevertheless, it needs to be ensured that the switch is performed safely, this means that the value of the Lyapunov function has to be globally decreasing along the *dwell time* (k_{dw}):

$$V_{\sigma_1}(x_k, \gamma) > V_{\sigma_2}(x_{k+k_{dw}}, \gamma) \tag{24}$$

In Figure 3, the evolution of the switching signal is shown. It can be seen that when the vehicle is running at low speed, the first mode σ_1 with $\bar{A}_{CL_{\sigma_1}}(\gamma)$ and the $G_{\sigma_1}^{-1}$ matrix defining the Lyapunov function of the closed-loop system is active. Then, when the vehicle increases its speed, the overlapping region is reached. Nevertheless, the first mode is active until the switching surface $\mathcal{S}_{12}$ is reached. If the controller switching fulfills (24), the LPV closed-loop switched system is ensured to be stable. This is translated into the following condition

$$x_k^T G_{\sigma_1}^{-1}(\gamma) x_k - x_{k+k_{dw}}^T G_{\sigma_2}^{-1}(\gamma) x_{k+k_{dw}} > 0 \tag{25}$$

or equivalently,

$$x_k^T (G_{\sigma_1}^{-1}(\gamma) - \bar{A}_{CL_{\sigma_1}}^{k_{dw}}(\gamma) G_{\sigma_2}^{-1}(\gamma) \bar{A}_{CL_{\sigma_1}}^{k_{dw}}) x_k > 0 \tag{26}$$

where $\bar{A}_{CL_\sigma}^{k_{dw}}(\gamma) = \prod_{d=k}^{d=k_{dw}} \bar{A}_{CL_\sigma}(\gamma_d)$. Via Schur complement [22], the following LMI is obtained

$$\begin{bmatrix} G_{\sigma_2}^{-1}(\gamma) & \bar{A}_{CL_{\sigma_1}}^{k_{dw}} \\ \star & G_{\sigma_1}(\gamma) \end{bmatrix} \succ 0 \tag{27}$$

In a similar way, when the vehicle is traveling at high speed, the second mode σ_2 with $\bar{A}_{CL_{\sigma_2}}(\gamma)$ and G_{σ_2} is active. If then the vehicle decelerates, the switch will be performed if the switching surface $\mathcal{S}_{21}$ is reached, and the following

LMI must hold in order to ensure the global decrease of the discontinuous Lyapunov function:

$$\begin{bmatrix} G_{\sigma_1}^{-1}(\gamma) & \bar{A}_{CL_{\sigma_2}}^{k_{dw}} \\ \star & G_{\sigma_2}(\gamma) \end{bmatrix} \succ 0 \tag{28}$$

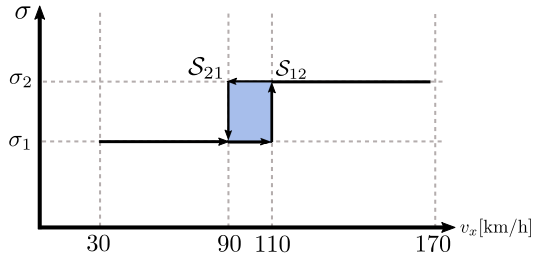

Fig. 3: Hysteresis switching strategy

In practice, the switching strategy is based on the parameter γ, defined by the vehicle speed. This means that the parameter variation is delimited by the maximal acceleration capabilities of the vehicle. In this way, once the subspace regions are defined and the respective closed-loop controllers are designed (19), the closed loop dynamics are known along the dwell time, and inequalities (27), (28) can be verified in a straightforward manner.

VI. Numerical Simulation

A numerical simulation is depicted in the following in order to show the performance of the switched LPV observer-based controller proposed in the previous sections in the presence of speed variations and curved roads. In Figure 4, the family of ellipsoids $G_\sigma^{-1}(\gamma)$ for the LCA system with two switching modes is shown by means of projections on the $(x_1, x_2), (x_3, x_4), (x_5, x_6)$-subspaces respectively (13). Such projections are also ellipsoids E_x [29] and are obtained through a suitable projection matrix T, $E_x = \{\bar{x}^T (T G_\sigma T^T)^{-1} \bar{x} \leq 1,\ \bar{x} = Tx\}$. These results have been obtained using the open-source programming framework YALMIP [30] and the optimization solver SEDUMI [31].

Figure 4 also shows the time trajectories of the system states in a scenario which is initiated at a perturbed state out of the computed RPI. The speed variation and road curvature used for the simulation are shown in Figure 5.

It can be seen Figure 7 that the value of the Lyapunov function is increasing at certain periods of time. This is due to the effect of the additive disturbances (curvature of the road) when the system state is inside the minimal Robust Positive Invariant Set [32], where the impact of the uncertainty cannot be completely counteracted. Finally, if we zoom-in it can be seen that the value of the Lyapunov function is globally decreasing due to the existence of a dwell-time imposed implicitly by the hysteresis mechanism for the switch.

VII. Concluding Remarks and Future Work

Considering the ADAS framework, LCA system has been described by means of an LPV polytopic representation of the system dynamics, considering the vehicle speed as a

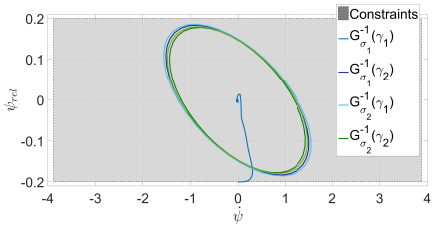

(a) Proy$(\dot{\psi}, \psi_{rel})$ plane

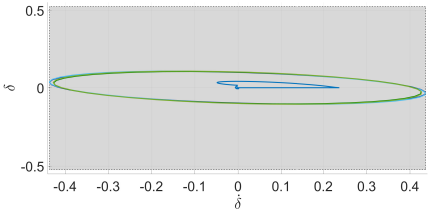

(b) Proy$(\dot{\delta}, \delta)$ plane

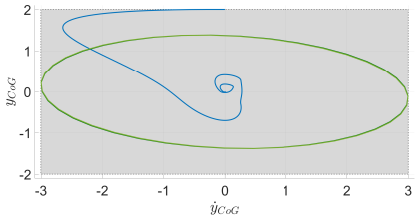

(c) Proy$(\dot{y}_{CoG}, y_{CoG})$ plane

Fig. 4: System states trajectories

bounded and measured parameter. Moreover, curvature of the road has been described by means of a parameter-varying additive disturbance, which has been bounded taking into account road design standards. Once the system has been delimited, the design of an ISS LPV observer-based controller design that maximizes the size of the RPI set, taking into account input, output and internal states constraints has been proposed. In addition to this, a LPV switched control strategy has been used to reduce the conservativeness introduced by the large range of speed variation. Numerical simulations on an example scenario have been provided, showing the proposed solution performance in the presence of both speed and curvature variations. Further directions will be oriented to carry out tests of the proposed estimation and control tuning on prototype experiments.

Acknowledgment

The work leading to these results has received funding from the People Programme (Marie Curie Actions) of the European Unions Seventh Framework Programme (FP7/2007-2013) under REA grant agreement no 607957 (TEMPO).

References

[1] R. Behringer, S. Sundareswaran, B. Gregory, R. Elsley, B. Addison, W. Guthmiller, R. Daily, and D. Bevly, "The DARPA grand challenge-development of an autonomous vehicle," in *Intelligent Vehicles Symposium, 2004 IEEE*. IEEE, 2004, pp. 226–231.

[2] V. der Automobilindustrie eV, "Automation: From driver assistance systems to automated driving," *VDA Magazine-Automation*, 2015.

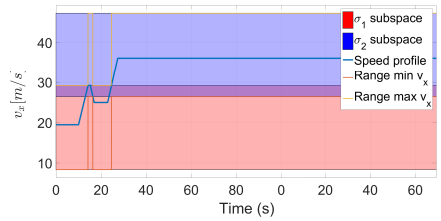

(a) Speed simulation profile. The switching signal σ_j exhibits three switches along the simulation, which can be identified with the changes on the range of speed variation.

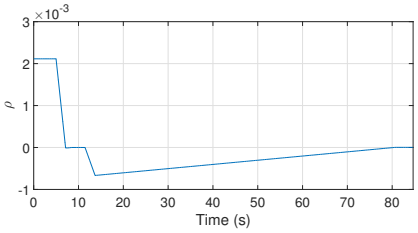

(b) Curve simulation profile

Fig. 5: Simulation Conditions

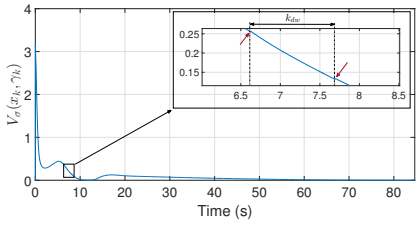

Fig. 6: Lyapunov function $V_\sigma(x_k, \gamma_k)$ time evolution

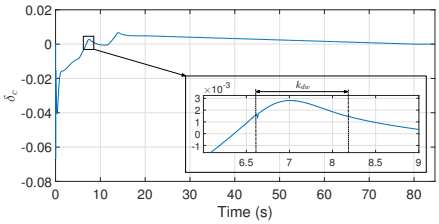

Fig. 7: Input trajectory

[3] N. M. Enache, "Assistance préventive à la sortie de voie," Ph.D. dissertation, Université d'Evry-Val d'Essonne, 2008.

[4] K. D. Kusano and H. C. Gabler, "Safety benefits of forward collision warning, brake assist, and autonomous braking systems in rear-end collisions," *IEEE Transactions on Intelligent Transportation Systems*, vol. 13, no. 4, pp. 1546–1555, 2012.

[5] E. Coelingh, A. Eidehall, and M. Bengtsson, "Collision warning with full auto brake and pedestrian detection-a practical example of automatic emergency braking," in *Intelligent Transportation Systems (ITSC), 2010 13th International IEEE Conference on*. IEEE, 2010, pp. 155–160.

[6] A. Vahidi and A. Eskandarian, "Research advances in intelligent collision avoidance and adaptive cruise control," *IEEE transactions on intelligent transportation systems*, vol. 4, no. 3, pp. 143–153, 2003.

[7] P. Falcone, F. Borrelli, J. Asgari, H. E. Tseng, and D. Hrovat, "Predictive active steering control for autonomous vehicle systems," *Control Systems Technology, IEEE Transactions on*, vol. 15, no. 3, pp. 566–580, 2007.

[8] R. Rajamani, *Vehicle dynamics and control*. Springer, 2006, ch. 2 Lateral Vehicle Dynamics.

[9] K. A. Brookhuis, D. De Waard, and W. H. Janssen, "Behavioural impacts of advanced driver assistance systems–an overview," *EJTIR*, vol. 1, no. 3, pp. 245–253, 2001.

[10] I. Ballesteros-Tolosana, S. Olaru, P. Rodriguez-Ayerbe, G. Pita-Gil, and R. Deborne, "Comparison of optimization-based strategies for constrained control of Auto-Steering systems," in *Control Conference (ECC), 2016 European*. IEEE, 2016, pp. 1592–1597.

[11] R. Schubert, K. Schulze, and G. Wanielik, "Situation assessment for automatic lane-change maneuvers," *IEEE Transactions on Intelligent Transportation Systems*, vol. 11, no. 3, pp. 607–616, 2010.

[12] O. Sename, P. Gaspar, and J. Bokor, *Robust control and linear parameter varying approaches: application to vehicle dynamics*. Springer, 2013, vol. 437.

[13] R. N. Jazar, *Vehicle dynamics: theory and application*. Springer Science & Business Media, 2013.

[14] H. Pacejka, *Tire and vehicle dynamics*. Elsevier, 2005.

[15] S. Di Cairano, H. E. Tseng, D. Bernardini, and A. Bemporad, "Vehicle yaw stability control by coordinated active front steering and differential braking in the tire sideslip angles domain," *Control Systems Technology, IEEE Transactions on*, vol. 21, no. 4, pp. 1236–1248, 2013.

[16] P. Falcone, F. Borrelli, J. Asgari, H. E. Tseng, and D. Hrovat, "A real-time model predictive control approach for autonomous active steering," *Nonlinear Model Predictive Control for Fast Systems, Grenoble, France*, 2006.

[17] O. Hanke, T. Bertram, and M. Hiller, "Analysis and control of vehicle dynamics under crosswind conditions," in *Advanced Intelligent Mechatronics, 2001. Proceedings. 2001 IEEE/ASME International Conference on*, vol. 1. IEEE, 2001, pp. 331–336.

[18] M. Vertet and S. Giausserand, *Comprendre les principaux paramètres de conception géométrique des routes*. Sétra, 2006.

[19] I. Ballesteros-Tolosana, S. Olaru, P. Rodriguez-Ayerbe, M. Hovd, G. Pita-Gil, and R. Deborne, "On the impact of additive disturbances on Auto-Steering systems," in *Accepted on IFAC World Congress, Toulouse*, 2017.

[20] J. Reimpell, H. Stoll, and J. Betzler, *The automotive chassis: engineering principles*. Butterworth-Heinemann, 2001.

[21] J. Ackermann, *Robust control: Systems with uncertain physical parameters*. Springer Science & Business Media, 2012.

[22] S. Boyd, L. El Ghaoui, E. Feron, and V. Balakrishnan, *Linear matrix inequalities in system and control theory*. SIAM, 1994.

[23] A. Luca, P. Rodriguez-Ayerbe, and D. Dumur, "Control of disturbed LPV systems in a LMI setting," *IFAC Proceedings Volumes*, vol. 44, no. 1, pp. 4149–4154, 2011.

[24] M. Kocvara, M. Stingl, and P. GbR, "PENBMI users guide (version 2.1)," *software manual, PENOPT GbR, Hauptstrasse A*, vol. 31, p. 91338, 2005.

[25] H.-N. Nguyen, S. Olaru, P. O. Gutman, and M. Hovd, "Constrained control of uncertain, time-varying linear discrete-time systems subject to bounded disturbances," *IEEE Transactions on Automatic Control*, vol. 60, no. 3, pp. 831–836, 2015.

[26] M. V. Kothare, V. Balakrishnan, and M. Morari, "Robust constrained model predictive control using linear matrix inequalities," *Automatica*, vol. 32, no. 10, pp. 1361–1379, 1996.

[27] B. Lu and F. Wu, "Switching LPV control designs using multiple parameter-dependent Lyapunov functions," *Automatica*, vol. 40, no. 11, pp. 1973–1980, 2004.

[28] B. Lu, F. Wu, and S. Kim, "Switching LPV control of an F-16 aircraft via controller state reset," *IEEE transactions on control systems technology*, vol. 14, no. 2, pp. 267–277, 2006.

[29] F. Blanchini and S. Miani, *Set-theoretic methods in control*. Springer, 2008.

[30] "YALMIP: A toolbox for modeling and optimization in MATLAB, author=Lofberg, Johan, booktitle=Computer Aided Control Systems Design, 2004 IEEE International Symposium on, pages=284–289, year=2005, organization=IEEE."

[31] Y. Labit, D. Peaucelle, and D. Henrion, "SeDuMi interface 1.02: a tool for solving LMI problems with SeDuMi," in *Computer Aided Control System Design, 2002. Proceedings. 2002 IEEE International Symposium on*. IEEE, 2002, pp. 272–277.

[32] S. Olaru, J. De Doná, M. Seron, and F. Stoican, "Positive invariant sets for fault tolerant multisensor control schemes," *International Journal of Control*, vol. 83, no. 12, pp. 2622–2640, 2010.